Jurnal Kejuruteraan 37(7) 2025: 3075-3087
https://doi.org/10.17576/jkukm-2025-37(7)-01

Optimization of Process Parameters with the Taguchi Method for Best Build Time and Surface Quality

Thavinnesh Kumar Rajendran, Mohd Afiq Shahrum, Shajahan Maidin* & Shafinaz Ismail

Faculty of Industrial & Manufacturing Technology & Engineering,
Universiti Teknikal Malaysia Melaka, Melaka, Malaysia

**Corresponding author: shajahan@utem.edu.my*

Received 2 January 2025, Received in revised form 22 June 2025
Accepted 22 July 2025, Available online 30 October 2025

ABSTRACT

Taguchi Method is a valuable tool that has been introduced to optimize the quality of products or processes. It effectively identifies the optimal combination with a minimal number of experiments. In the case of parts printed with Fused Deposition Modeling printers, the outcomes vary depending on changes in the printer process parameters, such as build orientation, layer thickness, and raster angles. This study focused on samples produced using Stratasys FDM 400 FDM 3D printer, evaluating their build time and surface roughness performance. To achieve optimal performance, the Taguchi Method was applied. For this project, an $L_9(3^3)$ orthogonal array was employed, involving 9 sample pieces printed with ABS-M30i material to assess three parameters, namely build orientation, layer thickness, and raster angles, each at three different levels. The samples (mounting bracket) were designed with SolidWorks. They were then evaluated for build time and tested for surface roughness using the Mitutoyo Surftest SJ 301. The resulting data was analyzed, revealing that the samples with an XY orientation, a layer thickness of 0.33 mm, and a raster angle of 90° achieved the shortest build time. Conversely, the samples with an XY orientation, a layer thickness of 0.18 mm, and a raster angle of 30° demonstrated the lowest average surface roughness (Ra value). These findings indicate that the properties of samples produced with the Stratasys FDM 400 MC printer vary depending on the combination of process parameters.

Keywords: Fused Deposition Modeling; Taguchi Method; ABS-M30i; process parameters; build time; surface roughness

INTRODUCTION

Additive manufacturing (AM) is one of the advanced manufacturing technologies used to create objects layer by layer straight from a computer-aided design (CAD) file. AM enables the creation of customized designs. Therefore, form complexity is not an issue. Compared to the conventional process, using AM to create the part takes less time. Furthermore, because no tooling is required, AM products are less expensive. Fused deposition modelling (FDM) is one of the most extensively used additive manufacturing systems (Gibson et al. 2021; Kumar & Prasad 2021). Molten material systems heat the system to melting temperature, allowing the molten material to flow through the nozzle for controlled distribution. The extrusion technique is used to get the material out of the nozzle. The systems will include two extrusion heads. This allows for the construction of support structures from various materials and the proper removal of support structures (Lalegani Dezaki et al. 2021).

The heating chamber is one of the instruments used in FDM to allow for the liquefaction of molten materials. Then, they are introduced into the system as a filament. A tractor-wheel arrangement is utilized to propel the filament into the chamber. Extrusion pressure is generated, causing the plastic to flow through the nozzle (Hu & Qin 2020).

FDM is a method that begins with liquefying thermoplastics or wax material and depositing it layer by layer through an extrusion nozzle. The material required to construct the item is often given in the form of a filament or metal wire (Baechle-Clayton et al. 2022; Sathies et al. 2020). After that, a coil of metal or plastic filament would be unravelled. Subsequently, the material would be fed into an extrusion nozzle, allowing the flow to be turned on and off to deposit the layers (Quero et al. 2021). To melt the plastics, the nozzle is heated to a temperature slightly above

the melting point. This ensures that the plastic flows smoothly through the nozzle and that the layers are correctly formed (Mallikarjuna et al. 2023). CAM software can control the nozzle's movement in both horizontal and vertical directions. The layers will solidify immediately after leaving the nozzle. They will adhere to the layer beneath it. Once a layer has been constructed, the platform will be lowered, and the extrusion nozzle will begin to deposit the next layer (Aruna Prabha et al. 2021; Scapin & Peroni, 2021; Xiao et al. 2021).

Materials suitable for the FDM technique include ABS plastic, investment casting wax, medical-grade ABS thermoplastics, and elastomers. Support materials are typically filaments with a diameter of around 0.070 inches and are rolled up on spools. The support material is easy to remove using a knife or pliers (Arefin et al. 2021). FDM parts are more robust, stronger, resistant to chemicals, moisture, and heat, and environmentally friendly. Because they are environmentally stable, FDM parts do not fluctuate in response to changes in surrounding temperature (Wickramasinghe et al. 2020). There are many different varieties of FDM materials, each with its own set of features, such as ABS, PLA, and polypropylene or PP (Kristiawan et al. 2021).

FDM is used to create prototype models that are utilized for early observation and functional testing of a design (Garzon-Hernandez et al. 2020; Sathishkumar et al. 2020). It can also be used to make direct-use components like jigs and fixtures. In addition, FDM can be used for investment casting and injection moulding. FDM can produce prototypes almost identical to the moulded product (Montez et al. 2022). Furthermore, using ABS material, FDM prototypes can be as strong as the moulded product. This will make it easier to construct fast prototypes for functional testing (Rodríguez-Reyna et al. 2022; Romero et al. 2021). FDM parts are created by extruding liquefied plastic through an extrusion nozzle layer by layer. As a result, only the material required to produce the item will be melted and placed. Hence, material wastes will be limited to a minimum level (DePalma et al. 2020; Suárez & Domínguez 2020).

FDM parts will take longer to produce than other processes. This is mainly because FDM-produced pieces must be filled with ABS materials. The extrusion rate has the most significant impact on building speed. If the extrusion rate is slow, the building pace is reduced, and the parts take longer to manufacture. The part is made of ABS thermoplastics. ABS material has relatively high viscosities; therefore, construction speed cannot be enhanced. (Baechle-Clayton et al. 2022b). Parts manufactured using FDM will exhibit random shrinking. This is because, after the components have been formed, the quick cooling of the material causes tension on the parts. As a result, the material density will drop, reducing the density of the part. As a result, customers must put in extra effort to compensate for unforeseen shrinkage by modifying the FDM machine's process parameters (Rosli et al. 2020).

FDM is a printing method that is increasingly being employed in medical applications. It builds custom implants, prosthetics, and anatomical models by adding thermoplastic materials layer by layer. FDM's precision, cost-effectiveness, and capacity to manufacture patient-specific devices improve surgical planning, medical training, and personalized healthcare solutions (Haryńska et al. 2020). Likewise, FDM is widely utilized in the automotive sector for rapid prototyping, tooling, and the production of specialized parts. It enables the production of strong, lightweight components such as brackets, fittings, and interior pieces. FDM's capacity to rapidly generate functioning prototypes speeds up design iteration, testing, and innovation in automobile engineering, lowering development time and costs (Nayeem et al. 2023; Yadav et al. 2020).

AM technology, such as FDM, is being used in the aerospace industry to lower the cost of tools, materials, and labour. AM technology can eliminate the requirement for tooling and machining. Furthermore, design flexibility can be achieved because AM technology allows for easy design changes to achieve strong design levels. AM technology has decreased the time required for complex manufacturing processes in the aerospace industry, greatly decreasing the lead time (Karkun & Dharmalinga 2022).

The Taguchi method is a tool for design optimization. It is commonly utilized in product design and process optimization. When designing experiments, the Taguchi method is used to simplify the experimental plan and determine the feasibility of studying the interactions between various process parameters. This is especially crucial for quick prototyping because the cost of producing prototypes is relatively high. The Taguchi method will generally offer an experimental design as an orthogonal array, resulting in different combinations of parameters and levels in each trial. This study will look at three essential process parameters for Taguchi optimization: part orientation, layer thickness, and raster angles (Hikmat et al. 2021).

METHODOLOGY

PHASE 1: DETAIL DESIGN

Mounting brackets were created using Solidwork CAD software and must be optimized for built orientation, layer thickness, and raster angles. The mounting bracket was chosen as the design sample because it allows for a clear

assessment of the raster angle and layer thickness. Furthermore, the chosen samples meet the surface roughness measurement standards, which require a minimum distance of more than 4mm. Figure 1 depicts the detailed design of the mounting bracket, including dimensions.

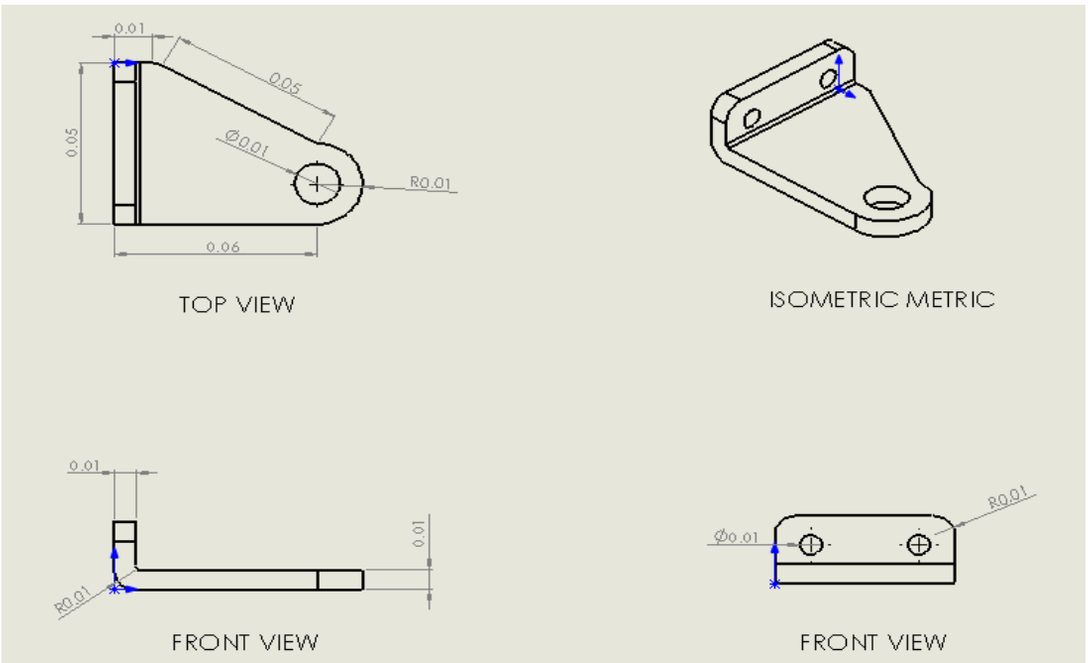

FIGURE 1. Detail design of Mounting Bracket with dimensions

PHASE 2: PREPARATION OF SAMPLES

Following the completion of the mounting bracket design in Phase One, the CAD drawing is converted into STL file format. This format is required because Additive Manufacturing (AM) machines accept only STL files, which they slice into thin cross-sectional layers for printing. Each AM machine has unique configuration settings tailored to its specific process. Therefore, once the STL file is transferred to the FDM machine, the printing parameters must be configured according to the values listed in Table 1.

After configuring the machine, the part is manufactured automatically. However, the fabrication process must be monitored carefully to prevent disruptions such as power outages or material shortages. Once the manufacturing process is complete, the printed part is removed from the machine, and the build time is recorded. Surface roughness of the samples is then assessed using the Mitutoyo Surftest SJ-301, and structural differences are observed under a Meiji Stereo Microscope.

It is crucial to understand the FDM machine's operation and its standard operating procedures (SOP) to avoid misuse, which could lead to equipment failure. The samples are fabricated using a Stratasys FDM 400 MC printer, as shown in Figure 2(a). Post-fabrication, the samples are placed in an ultrasonic tank containing SR-30, a soluble support material formulated explicitly for ABS-M30i thermoplastics, as illustrated in Figure 2(b). SR-30 is a synthetic thermoplastic polymer compatible with the Stratasys FDM 400 MC system and effectively dissolves support structures.

Nine sets of printing parameters, generated using orthogonal arrays in Minitab Software 17, are outlined in Table 2. Each sample is fabricated on the FDM 400 MC using one of these parameter combinations. The resulting nine mounting brackets are presented in Figure 2(c). After printing, the surface roughness of each bracket is measured using the Mitutoyo Surftest SJ-301, as depicted in Figures 2(d) and 2(e). Subsequently, the printed brackets are examined for structural characteristics using the Meiji Stereo Microscope, as shown in Figure 2(f).

TABLE 1. List of parameters with their values at each level.

Parameters	Symbol	Level 1	Level 2	Level 3
Build Orientation	A	XY	XZ	YZ
Layer thickness (mm)	B	0.18	0.25	0.33
Raster Angle (^{0})	C	30^0	45^0	90^0

TABLE 2. List of parameters with their values at each level

Sample	Parameters and Levels		
	A	B	C
1	1	1	1
2	1	2	2
3	1	3	3
4	2	1	2
5	2	2	3
6	2	3	1
7	3	1	3
8	3	2	1
9	3	3	2

(a)

(b)

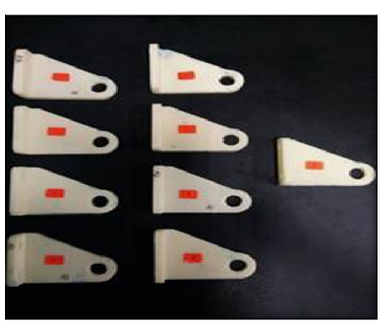

(c)

(d)

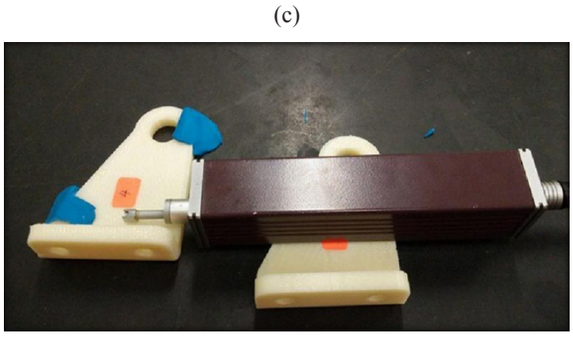

(e)

(f)

FIGURE 2. (a) Stratasys FDM 400 MC machine, (b) Ultrasonic tank with SR-30, (c) Printed mounting brackets, (d) Surface roughness measurement, (e) Touch probe on the sample, (f) Meiji Stereo Microscope.

PHASE 3: DATA COLLECTION

The varied parameter selections will result in parts with varying build times and surface roughness. When the part is completely created, the construction time can be determined, and the surface roughness can be measured with the Mitutoyo Surftest SJ-301.

PHASE 4: RESULT AND ANALYSIS

The design of the experiment, or DOE, was used at this stage to assist in planning relevant experiments with the parameters selected. Orthogonal Arrays can be used to create combinations of various parameters. The experiment was designed using Taguchi methodology to determine combinations and the number of runs required. The optimal combinations of the various parameters for build time and surface roughness are then determined.

RESULTS AND DISCUSSION

PARAMETER COMBINATION

Table 3 displays the various parameter combinations created using the Taguchi technique in the Minitab 17 software and shows the results of an experimental run with various parameter combinations acquired using the Minitab 17 software. Three critical parameters, build orientation, layer thickness, and raster angle, were investigated for their effect on response characteristics such as build time and surface roughness.

TABLE 3. Different combinations of parameter settings for each experimental run

Experimental Run	Parameter Combination	Parameters		
		Build Orientation	Layer Thickness (mm)	Raster Angle (^{0})
1	111	XY	0.18	30
2	122	XY	0.25	45
3	133	XY	0.33	90
4	212	XZ	0.18	45
5w	223	XZ	0.25	90
6	231	XZ	0.33	30
7	313	YZ	0.18	90
8	321	YZ	0.25	30
9	332	YZ	0.33	45

BUILD TIME

ANALYSIS OF DATA

Table 4 shows that the different parameter settings for experimental run 3 with the combination of XY orientation, layer thickness of 0.33 mm, and raster angle of 90° have the shortest build time of 49 minutes, followed by experimental runs 2 and 1. Experimental run 2 takes 63 minutes to create with an XY orientation, layer thickness of 0.25 mm, and raster angle of 45°. In contrast, experimental run 1 takes 107 minutes with an XY orientation, layer thickness of 0.18 cm, and raster angle of 30°.

On the flip side, the different combination of parameter settings for experimental run 7 with YZ orientation, layer thickness of 0.18 mm, and raster angle of 90° has the longest build time of 323 minutes, followed by experimental runs 4 and 8. Experimental run 4 takes 250 minutes to create with an XZ orientation, layer thickness of 0.18 mm, and raster angle of 45°. In contrast, experimental run 8 takes 198 minutes with a YZ orientation, layer thickness of 0.25 mm, and raster angle of 30°.

Based on the examination of construction time, experimental runs 1, 2, and 3 have a relatively lower build time than other experimental runs. They share the same XY construction orientation. As a result, XY orientation may produce a part faster than XZ and YZ orientations. As a result, experimental run 3 with the XY orientation, layer thickness of 0.33 mm, and raster angle of 90° has the quickest build time for a mounting bracket. Figure 3 shows that each experimental run has its own build time based on the many combinations of parameter settings that have been determined using the Taguchi design. The build time is noted to be shorter in some experimental runs but longer in others. This demonstrates that different combinations of parameter settings affect the build time of the printing process.

TABLE 4. Build Time Result for mounting brackets

Experimental Run	Combination	Build Orientation	Layer Thickness (mm)	Raster Angle (^{0})	Build Time (Minutes)
1	111	XY	0.18	30	107
2	122	XY	0.25	45	63
3	133	XY	0.33	90	49
4	212	XZ	0.18	45	250
5	223	XZ	0.25	90	151
6	231	XZ	0.33	30	119
7	313	YZ	0.18	90	323
8	321	YZ	0.25	30	198
9	332	YZ	0.33	45	159

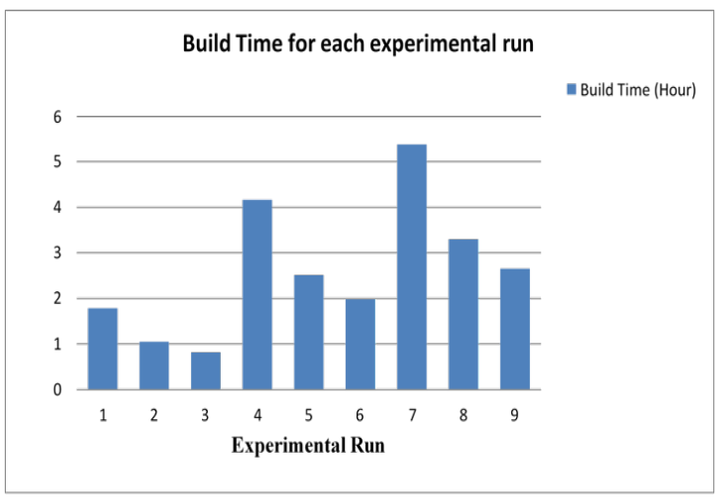

FIGURE 3. Build time for each experimental run

ANOVA ANALYSIS

An analysis of variance (ANOVA) can be performed to determine the relevance of parameters and their percentage contribution to the printers' build time. The three parameters to be optimized in this project are build orientation, layer thickness, and raster angle. Table 5 displays the percentage contributions of build orientation, layer thickness, and raster angle to build time.

The information from the pie chart in Figure 4 demonstrates that construction direction has a 58.57% effect on build time, followed by layer thickness (36.28%). Raster angle and inaccuracy have no substantial effect on build time, with the former accounting for 2.62% and the latter for only 2.53%. An ANOVA analysis is performed, and the F-value and p-value are used to determine the significant factor.

TABLE 5. Percentage contributions of parameters on build time

Parameters	Sum of Square	Percent Contribution (%)
Build Orientation	10.15	58.57
Layer Thickness	6.28	36.28
Raster Angle	0.45	2.62
Error	0.44	2.53
Total	17.32	100

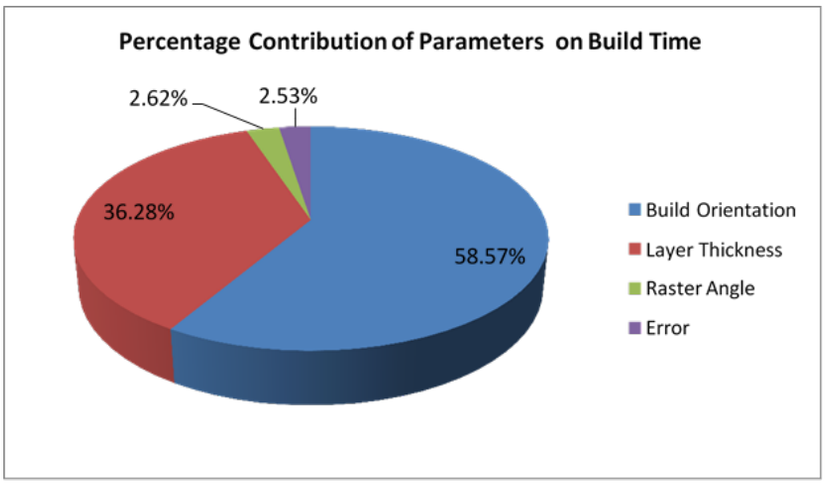

FIGURE 4. Percentage contributions of parameters on build time

Figure 5 presents a Pareto chart for building duration, demonstrating that build orientation is the most significant element influencing build time. In reality, build orientation has the most significant impact on the build time of the part printed. This data is consistent with the (Mishra & Thirumavalavan 2014). Observation that build orientation has the greatest influence on the build time of a part printed using FDM (Mishra & Thirumavalavan 2014). Different building orientations will result in the creation of a support structure. As a result, the support structure will appear in some orientations, making it take longer to fabricate the brackets.

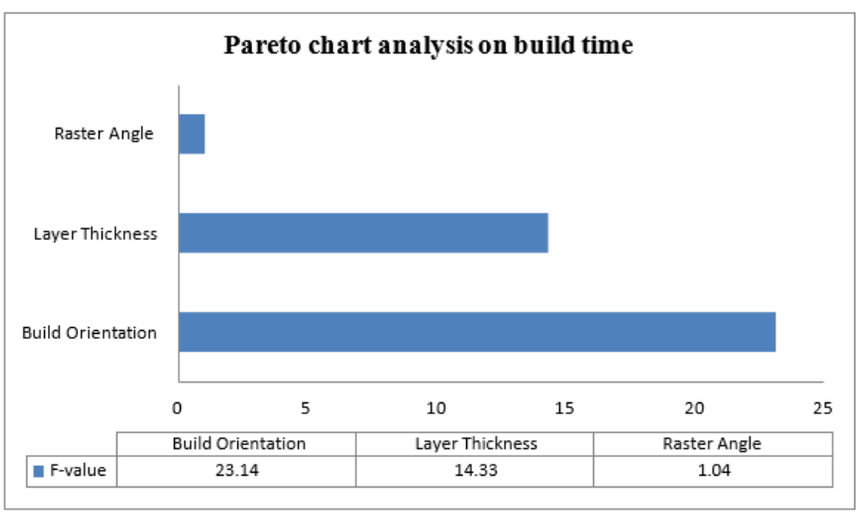

FIGURE 5. Pareto Chart on build time

As displayed in Figure 5, the F-value for build orientation and layer thickness is high. As a result, validation is required using p-value analysis to determine the significance parameters influencing build time. The P-value analysis was done using Minitab 17 software and is reported in Table 6. Table 6 indicates that only construction orientation substantially impacts build time, as the P-value (0.041) is lower than the α value (0.05). In addition, build orientation has a sufficiently high F-value when compared to layer thickness and raster angle. Usually, changing the process parameters affects the response characteristics. As a result, build orientation is the only parameter that substantially affects build time. It is confirmed with the P-value derived from Minitab 17 software.

TABLE 6. P-value analysis

Parameters	F-value	P-value	α value	Analysis	Significance
Build Orientation	23.14	0.041	0.05	P value < α value	Yes
Layer Thickness	14.33	0.065	0.05	P value > α value	No
Raster Angle	1.04	0.491	0.05	P value > α value	No

SURFACE ROUGHNESS

ANALYSIS OF DATA

The Roughness Average (Ra) value is the surface roughness parameter used in this investigation. Ra is the arithmetic mean of the absolute values of the roughness profile ordinates. Table 7 shows the surface roughness results for nine pieces generated.

TABLE 7. Surface Roughness Result for nine mounting brackets produced

Experimental Runs	Parameter Combination	Surface Roughness, Ra (μm)		
		1	2	Average Ra (μm)
1	111	0.37	0.21	0.553
		0.56	0.85	
		1.08	0.25	
2	122	1.19	1.05	1.097
		1.02	1.04	
		1.21	1.07	
3	133	1.22	1.19	1.195
		1.30	1.28	
		1.20	0.98	
4	212	0.85	0.71	0.710
		0.70	0.60	
		0.70	0.70	
5	223	1.31	1.25	1.177
		1.75	0.49	
		1.25	1.01	
6	231	1.81	0.92	1.430
		2.10	0.85	
		1.79	1.11	
7	313	0.69	0.69	0.708
		0.75	0.70	
		0.74	0.68	
8	321	1.79	0.43	1.178
		1.31	1.79	
9	332	1.25	2.01	1.570
		1.30	1.76	

Table 7 shows that experimental run 1 with XY orientation, layer thickness of 0.18 mm, and raster angle of 30° has the lowest average Ra value (0.553 μm), followed by experimental runs 7 and 4 with average Ra values of 0.708 μm and 0.710 μm, respectively. Experimental run 7 uses YZ orientation, layer thickness of 0.18 mm, and a raster angle of 90°, whereas experimental run 4 uses XZ orientation, layer thickness of 0.18 mm, and a raster angle of 45°.

Surface roughness research reveals three experimental runs with a lower average Ra value than the other runs. They share the same layer thickness of 0.18 mm. As a result, it can be determined that a layer thickness of 0.18 mm can provide a sample with lower surface roughness,

indicating higher surface quality. Experiment run 9 with YZ orientation, layer thickness of 0.33 mm, and raster angle of 45° had the highest average Ra value of 1.570 µm, followed by runs 6 and 3 with average Ra values of 1.430 µm and 1.195 µm. Experimental run 6 is a combination of XZ orientation, layer thickness of 0.33 mm, and raster angle of 30°, whereas experimental run 3 is a combination of XY orientation, layer thickness of 0.33 mm, and raster angle of 90°.

The average Ra value indicates that the part's surface quality improves as the average Ra value decreases. Thus, experimental run 1 with the combination of XY orientation, layer thickness of 0.18 mm, and raster angle of 300 may produce a sample with acceptable surface quality since it has the lowest average surface roughness, Ra value. For further examination, the data in Table 7 is turned into a histogram, as illustrated in Figure 6.

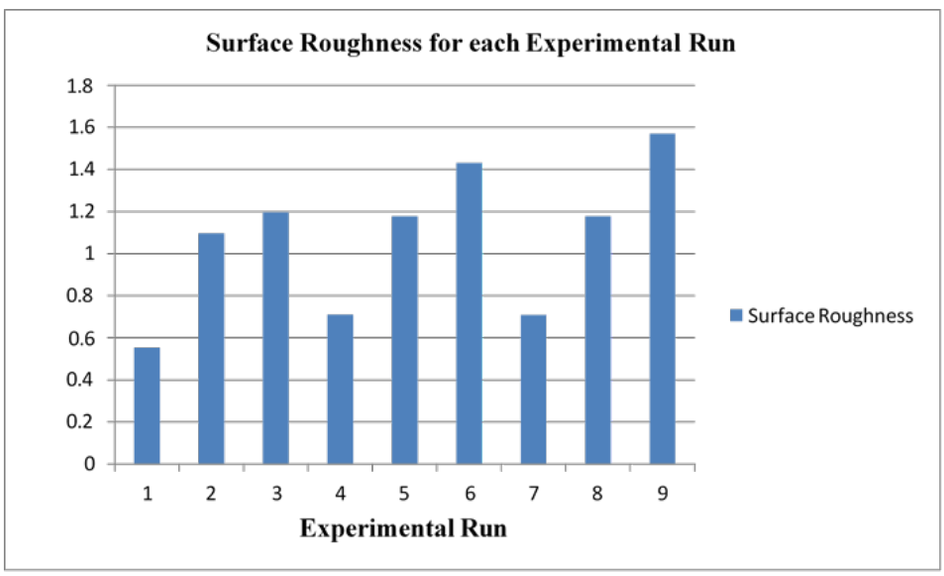

FIGURE 6. Average Surface Roughness, Ra value for each experimental run

MACROSCOPIC INSPECTION

A macroscopic inspection was carried out to examine the surface finish of the printed samples. Figure 7(a) illustrates that when using a low layer thickness of 0.18 mm, the spaces between layer deposition beads are 0.01mm. As a result, surface roughness diminishes, indicating improved surface quality.

Figure 7(b) demonstrates that when using a high layer thickness of 0.33 mm, the spaces between deposition beads are 0.02 mm. As a result, surface roughness increases, indicating a deterioration in surface quality. Therefore, when the layer thickness is reduced from 0.33 mm (high level) to 0.18 mm (low level), the voids between the deposition of material fall from 0.02 mm to 0.01 mm.

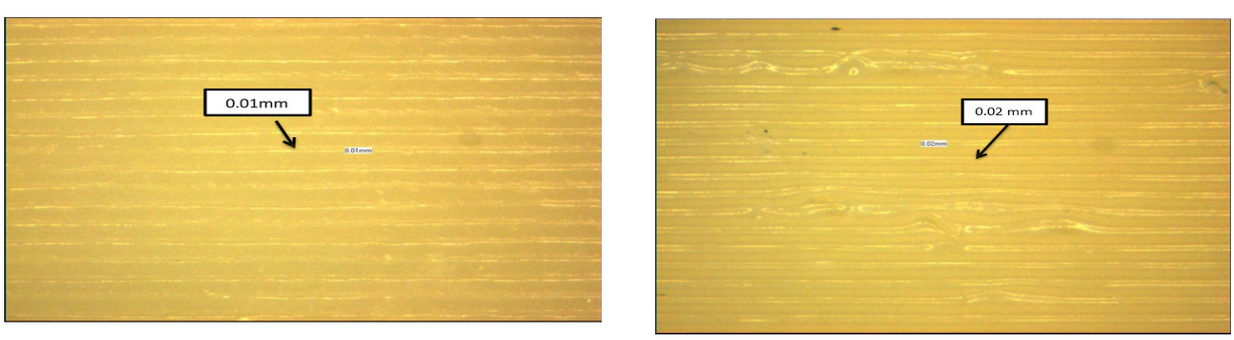

(a) (b)

FIGURE 7. (a) Experimental Run 1: XY orientation, 0.18 mm layer, 300° raster – lowest surface roughness, (b) Experimental Run 9: YZ orientation, 0.33 mm layer, 450° raster – highest surface roughness.

ANOVA ANALYSIS

The three parameters to be optimized in this research are build orientation, layer thickness, and raster angle. To determine the magnitude of each parameter's influence, the percentage contribution of each parameter's effect on surface roughness is calculated using Minitab 17 software. Table 8 shows the percentage contribution for each parameter, which is then summarised in a pie chart, as seen in Figure 8.

TABLE 8. Percentage contributions of parameters on surface roughness

Parameters	Sum of Square	Percent Contribution (%)
Build Orientation	0.068	7.22
Layer Thickness	0.855	90.25
Raster Angle	0.016	1.66
Error	0.008	0.87
Total	0.947	100

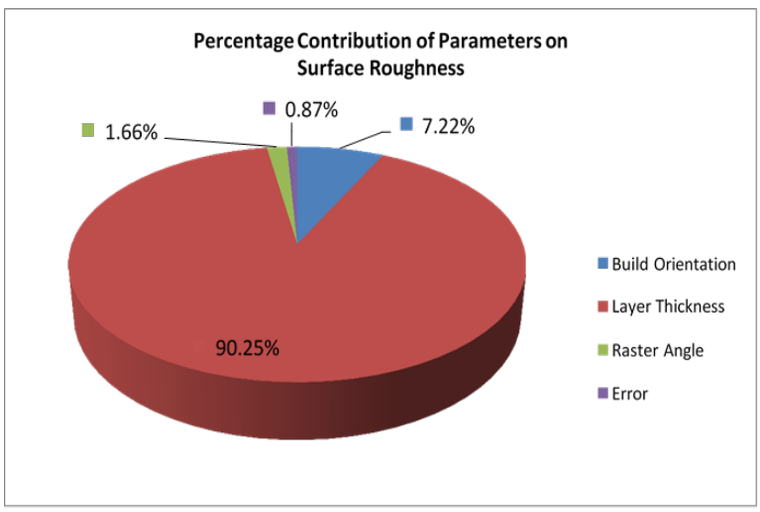

FIGURE 8. Percentage contributions of parameters on surface roughness

The pie chart in Figure 8 shows that layer thickness has a 90.25% effect on surface roughness, followed by build orientation at 7.22%. Raster angle and error have little effect on surface roughness, accounting for only 1.66% and 0.87%, respectively. An ANOVA analysis with F-value and P-value is performed to determine which factor is important.

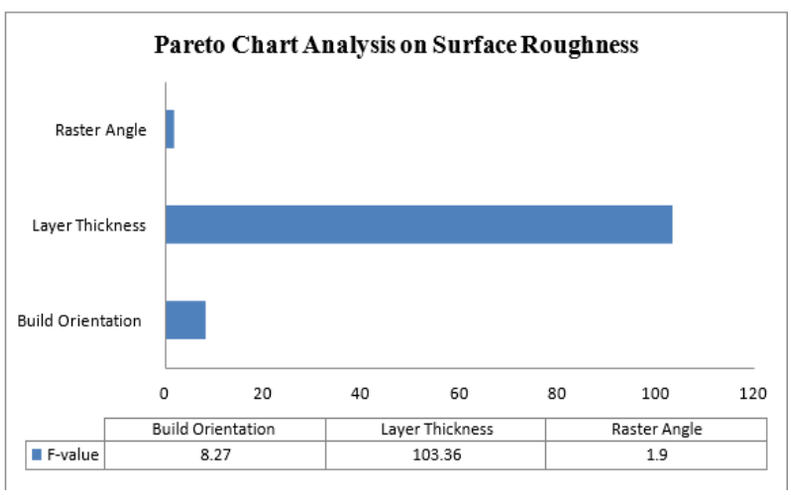

FIGURE 9. Pareto Chart on surface roughness

Figure 9 presents a Pareto chart for surface roughness, indicating that layer thickness is the most influential factor affecting surface quality. This finding aligns with the projection that layer thickness has the greatest impact on the surface roughness of FDM-printed parts, as also reported by (Nancharaiah et al. 2010).The chart shows a notably high F-value for layer thickness; however, further validation through p-value analysis is necessary to confirm these results. Table 9 provides the p-value analysis conducted using Minitab 17 software.

TABLE 9. P-value analysis

Parameters	F-value	P-value	α value	Analysis	Significance
Build Orientation	8.27	0.108	0.05	P value > α value	No
Layer Thickness	103.36	0.010	0.05	P value < α value	Yes
Raster Angle	1.90	0.345	0.05	P value > α value	No

Table 9 reveals that only layer thickness significantly affects surface roughness, with a P-value (0.01) less than the α value (0.05). Furthermore, layer thickness has a suitably high F-value relative to build orientation and raster angle. Usually, changing the process parameters affects the response characteristics. As a result, layer thickness is the only characteristic that substantially affects surface roughness. It is validated using the P-value derived from Minitab 17 software.

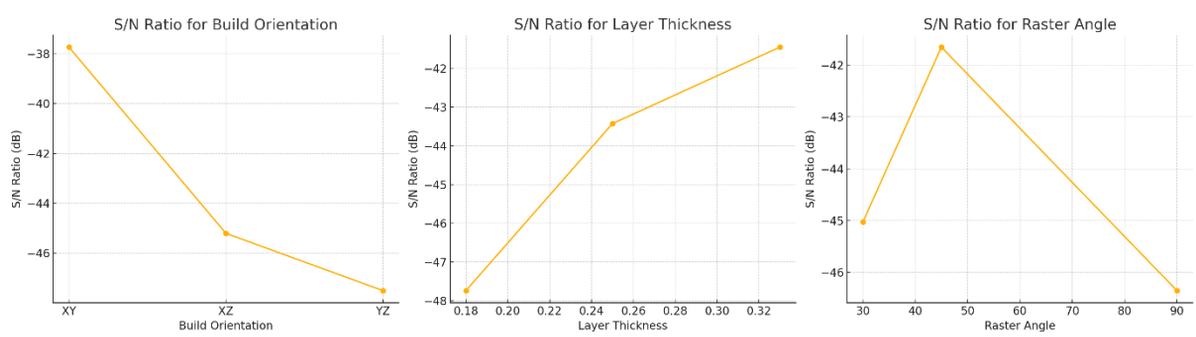

FIGURE 10. S/N ratio graphs for each factor

Based on the S/N ratio analysis using the Taguchi method in Figure 10, the factor that had the most favourable impact on minimizing build time was the build orientation, where the XY orientation exhibited the highest S/N ratio, indicating the shortest build time among the three orientations. In contrast, the YZ orientation resulted in the lowest S/N ratio, suggesting it leads to significantly longer build durations. Similarly, layer thickness played a crucial role in building efficiency. The 0.33 mm layer thickness showed the highest S/N ratio, making it the most effective for reducing build time, while the 0.18 mm layer produced the lowest S/N ratio and, thus, the longest build time. Finally, in terms of raster angle, the 45° angle emerged as the optimal setting with the best S/N ratio for minimizing build time, whereas the 90° raster angle corresponded to the lowest performance in this regard. Shorter build times are suggested to be achieved using a build orientation of XY, a layer thickness of 0.33 mm, and a raster angle of 45°.

CONCLUSION

In today's fast-paced manufacturing environment, additive manufacturing offers an efficient option for producing functional parts; however, performance variation remains a challenge. This study applied the Taguchi Method to optimize build orientation, layer thickness, and raster angle to minimize build time and improve surface quality.

Nine samples were fabricated using a mounting bracket sample printed with Stratasys FDM 400MC and ABS-M30i material through a design-of-experiments approach. The results identified that the XY orientation, 0.33 mm layer thickness, and 90° raster angle achieved the shortest build time, while the XY orientation, 0.18 mm layer thickness, and 30° raster angle produced the best surface finish.

ANOVA analysis confirmed that build orientation predominantly affects build time, whereas layer thickness significantly impacts surface roughness. The findings demonstrate the effectiveness of the Taguchi Method in optimizing FDM process parameters, leading to improved part quality and reduced production time and costs.

ACKNOWLEDGEMENT

This work was supported by the Universiti Teknikal Malaysia Melaka (UTeM) for awarding the Zamalah Scholarship.

DECLARATION OF COMPETING INTEREST

None.

REFERENCES

Arefin, A. M. E., Khatri, N. R., Kulkarni, N., & Egan, P. F. 2021. Polymer 3D Printing Review: Materials, Process, and Design Strategies for Medical Applications. *Polymers* 13(9): 1499. https://doi.org/10.3390/polym13091499

Aruna Prabha, K., Sai Rohit, P., Nitturi, S. C., & Nithin, B. 2021. Manufacturing of 3 D Shrouded Impeller of a Centrifugal Compressor on the 3D-Printing machine using FDM Technology. *IOP Conference Series: Materials Science and Engineering* 1012(1): 012039. https://doi.org/10.1088/1757-899X/1012/1/012039

Baechle-Clayton, M., Loos, E., Taheri, M., & Taheri, H. 2022a. Failures and Flaws in Fused Deposition Modeling (FDM) Additively Manufactured Polymers and Composites. *Journal of Composites Science* 6(7): 202. https://doi.org/10.3390/jcs6070202

Baechle-Clayton, M., Loos, E., Taheri, M., & Taheri, H. 2022b. Failures and Flaws in Fused Deposition Modeling (FDM) Additively Manufactured Polymers and Composites. *Journal of Composites Science* 6(7): 202. https://doi.org/10.3390/jcs6070202

DePalma, K., Walluk, M. R., Murtaugh, A., Hilton, J., McConky, S., & Hilton, B. 2020. Assessment of 3D printing using fused deposition modelling and selective laser sintering for a circular economy. *Journal of Cleaner Production* 264: 121567. https://doi.org/10.1016/j.jclepro.2020.121567

Garzon-Hernandez, S., Garcia-Gonzalez, D., Jérusalem, A., & Arias, A. 2020. Design of FDM 3D printed polymers: An experimental-modelling methodology for the prediction of mechanical properties. *Materials & Design* 188: 108414. https://doi.org/10.1016/j.matdes.2019.108414

Gibson, I., Rosen, D., Stucker, B., & Khorasani, M. 2021. Development of Additive Manufacturing Technology. In *Additive Manufacturing Technologies* (pp. 23–51). Springer International Publishing. https://doi.org/10.1007/978-3-030-56127-7_2

Haryńska, A., Carayon, I., Kosmela, P., Szeliski, K., Łapiński, M., Pokrywczyńska, M., Kucińska-Lipka, J., & Janik, H. 2020. A comprehensive evaluation of flexible FDM/FFF 3D printing filament as a potential material in medical application. *European Polymer Journal* 138: 109958. https://doi.org/10.1016/j.eurpolymj.2020.109958

Hikmat, M., Rostam, S., & Ahmed, Y. M. 2021. Investigation of tensile property-based Taguchi method of PLA parts fabricated by FDM 3D printing technology. *Results in Engineering* 11: 100264. https://doi.org/10.1016/j.rineng.2021.100264

Hu, C., & Qin, Q.-H. 2020. Advances in fused deposition modeling of discontinuous fiber/polymer composites. *Current Opinion in Solid State and Materials Science* 24(5): 100867. https://doi.org/10.1016/j.cossms.2020.100867

Karkun, M. S., & Dharmalinga, S. 2022. 3D Printing Technology in Aerospace Industry – A Review. *International Journal of Aviation, Aeronautics, and Aerospace*. https://doi.org/10.15394/ijaaa.2022.1708

Kristiawan, R. B., Imaduddin, F., Ariawan, D., Ubaidillah, & Arifin, Z. 2021. A review on the fused deposition modelling (FDM) 3D printing: Filament processing, materials, and printing parameters. *Open Engineerin* 11(1): 639–649. https://doi.org/10.1515/eng-2021-0063

Kumar, S. A., & Prasad, R. V. S. 2021. Basic principles of additive manufacturing: different additive manufacturing technologies. In *Additive Manufacturing* (pp. 17–35). Elsevier. https://doi.org/10.1016/B978-0-12-822056-6.00012-6

Lalegani Dezaki, M., Mohd Ariffin, M. K. A., & Hatami, S. 2021. An overview of fused deposition modelling (FDM): research, development and process optimization. *Rapid Prototyping Journal* 27(3): 562–582. https://doi.org/10.1108/RPJ-08-2019-0230

Mallikarjuna, B., Bhargav, P., Hiremath, S., Jayachristiyan, K. G., & Jayanth, N. 2023. A review on the melt extrusion-based fused deposition modelling (FDM): Background, materials, process parameters and military applications. *International Journal on Interactive Design and Manufacturing (IJIDeM)*. https://doi.org/10.1007/s12008-023-01354-0

Mishra, A. K., & Thirumavalavan, S. 2014. A Study of part orientation in rapid prototyping. *Middle East Journal of Scientific Research* 20: 1197–1201.

Montez, M., Willis, K., Rendler, H., Marshall, C., Rubio, E., Rajak, D. K., Rahman, M. H., & Menezes, P. L. (2022). Fused deposition modelling (FDM): processes, material properties, and applications. In *Tribology of Additively Manufactured Materials* (pp. 137–163). Elsevier. https://doi.org/10.1016/B978-0-12-821328-5.00005-6

Nancharaiah, T., Ranga Raju, D., & Ramachandra Raju, V. 2010. An experimental investigation on surface quality and dimensional accuracy of FDM components.

Nayeem, Abusaleh Md, & Mir Md Nasim Hossain. 2023. Usage of additive manufacturing in the automotive industry: A review. *International Journal of Accounting & Finance Review*, 9–20. https://doi.org/10.46281/bjmsr.v8i1.2135

Quero, R. F., Domingos da Silveira, G., Fracassi da Silva, J. A., & Jesus, D. P. de. 2021. Understanding and improving FDM 3D printing to fabricate high-resolution and optically transparent microfluidic devices. *Lab on a Chip*. 21(19): 3715–3729. https://doi.org/10.1039/D1LC00518A

Rodríguez-Reyna, S. L., Mata, C., Díaz-Aguilera, J. H., Acevedo-Parra, H. R., & Tapia, F. 2022. Mechanical properties optimization for PLA, ABS, and Nylon + CF manufactured by 3D FDM printing. *Materials Today Communications* 33: 104774. https://doi.org/10.1016/j.mtcomm.2022.104774

Romero, P. E., Arribas-Barrios, J., Rodriguez-Alabanda, O., González-Merino, R., & Guerrero-Vaca, G. 2021. Manufacture of polyurethane foam parts for automotive industry using FDM 3D printed molds. *CIRP Journal of Manufacturing Science and Technology* 32: 396–404. https://doi.org/10.1016/j.cirpj.2021.01.019

Rosli, A. A., Shuib, R. K., Ishak, K. M. K., Hamid, Z. A. A., Abdullah, M. K., & Rusli, A. 2020. Influence of bed temperature on warpage, shrinkage, and density of various acrylonitrile butadiene styrene (ABS) parts from fused deposition modelling (FDM). 020072. https://doi.org/10.1063/5.0015799

Sathishkumar, N., Udayakumar, A. S. M., Vincent, B., & Ashok Kumar, V. 2020. Study and analysis of 3D printed FDM components by non-destructive testing techniques. *International Journal of Research and Review (Ijrrjournal.Com)* 7(5): 5.

Scapin, M., & Peroni, L. 2021. Numerical Simulations of Components Produced by Fused Deposition 3D Printing. *Materials* 14(16): 4625. https://doi.org/10.3390/ma14164625

Suárez, L., & Domínguez, M. 2020. Sustainability and environmental impact of fused deposition modelling (FDM) technologies. *The International Journal of Advanced Manufacturing Technology* 106(3–4): 1267–1279. https://doi.org/10.1007/s00170-019-04676-0

T., S., P., S., & M.S., A. 2020. A review on advancements in applications of fused deposition modelling process. *Rapid Prototyping Journal* 26(4): 669–687. https://doi.org/10.1108/RPJ-08-2018-0199

Wickramasinghe, S., Do, T., & Tran, P. 2020. FDM-Based 3D Printing of Polymer and Associated Composite: A Review on Mechanical Properties, Defects and Treatments. *Polymers* 12(7): 1529. https://doi.org/10.3390/polym12071529

Xiao, J., Eynard, B., Anwer, N., Durupt, A., Le Duigou, J., & Danjou, C. 2021. STEP/STEP-NC-compliant manufacturing information of 3D printing for FDM technology. *The International Journal of Advanced Manufacturing Technology* 112(5–6): 1713–1728. https://doi.org/10.1007/s00170-020-06539-5

Yadav, D. K., Srivastava, R., & Dev, S. 2020. Design & fabrication of ABS part by FDM for automobile application. *Materials Today: Proceedings* 26: 2089–2093. https://doi.org/10.1016/j.matpr.2020.02.451